

# Self-interaction corrected electronic structure of $\text{Ti}_4\text{O}_7$ , $\text{TiO}_2$ and $\text{Ti}_2\text{O}_3$

X. Zhong,<sup>1</sup> I. Rungger,<sup>2</sup> P. Zapol,<sup>1</sup> and O. Heinonen<sup>1,3</sup>

<sup>1</sup>Materials Science Division, Argonne National Laboratory, Lemont, Illinois 60439, USA

<sup>2</sup>School of Physics, AMBER and CRANN, Trinity College, Dublin 2, Ireland

<sup>3</sup>Center for Hierarchical Materials Design, Northwestern University, 2145 Sheridan Rd, Evanston, IL 60208

(September 16, 2014)



## Abstract

We have studied three titanium oxides, rutile  $\text{TiO}_2$ ,  $\text{Ti}_2\text{O}_3$ , and Magnéli phase  $\text{Ti}_4\text{O}_7$ , using density functional theory with self-interaction corrections. We found that the ground state of the low temperature ( $T < 142$  K) phase (or LT phase) of  $\text{Ti}_4\text{O}_7$  is a new semiconducting state with antiferromagnetic coupling between two sublattices, while the high temperature (room temperature) phase (or HT phase) is a metal, in agreement with previous experiments. We have also investigated the dependence of electronic and magnetic properties of these Ti-O phases on the single empirical parameter  $\alpha$  representing the applied self-interaction correction. We show that Pauli paramagnetism of the metallic HT- $\text{Ti}_4\text{O}_7$  is predicted using  $\alpha \approx 0$ , that the band gaps of small-gap LT- $\text{Ti}_4\text{O}_7$  and  $\text{Ti}_2\text{O}_3$  are captured by  $\alpha \approx 0.5$ , while the band gap of wide-gap  $\text{TiO}_2$  is reproduced using  $\alpha \approx 0.9$ . The increasing value of  $\alpha$  for increasing value of the gap is consistent with increasing ionic bonding and decreasing screening. Nevertheless, restricting  $\alpha$  to the standard value for transition metal oxides of 0.5 is shown to be a good compromise describing reasonably well the electronic structures of these oxides. We also studied the effect of isotropic strain on  $\text{Ti}_4\text{O}_7$  electronic structure, and we predict an antiferromagnetic-ferromagnetic phase transition for the LT phase under compressive strain.



# 1. Introduction

Titanium dioxide ( $\text{TiO}_2$ ) is a binary oxide that has been extensively investigated for its applications in photovoltaics<sup>1</sup>, photocatalysis<sup>2</sup> and, recently, resistive switching<sup>3-5</sup>. A typical structure exhibiting resistive switching consists of a  $\text{TiO}_2$  layer sandwiched between two metal electrodes. The resistance can be switched between two distinctive resistive states by the application of voltage pulses. It is now firmly established that oxygen vacancies play a crucial role<sup>4, 6-8</sup> in the switching mechanism. Stoichiometric  $\text{TiO}_2$  can easily be reduced<sup>9, 10, 11</sup> by external fields or by thermal means, leading to oxygen-deficient phases. When the concentration of the resulting oxygen vacancies is high enough, these phases may rearrange spontaneously to form ordered reduced structures, the so-called Magnéli phases ( $\text{Ti}_n\text{O}_{2n-1}$ ). In fact, Magnéli phases such as  $\text{Ti}_4\text{O}_7$  ( $n=4$ ) have been identified experimentally<sup>6, 9</sup> in resistive switching devices, with evidence suggesting that filaments or regions of Magnéli phase  $\text{Ti}_4\text{O}_7$  form conducting pathways. The formation of conductive filaments leads to a low-resistance state of the device, while the rupture of filaments leads to a high-resistance state.

Understanding the resistive-switching behavior of  $\text{TiO}_2$ -based structures requires detailed knowledge of electronic properties of the different sub-stoichiometric phases of titanium oxide. From a theoretical and modeling point of view, it is known<sup>7, 12, 13</sup> that density functional theory (DFT) using the conventional local density approximation (LDA) or generalized gradient approximation (GGA) does not yield an accurate description of the electronic structure (e.g., band gap, or location of defect states within the band gap) of pristine and oxygen-deficient  $\text{TiO}_2$ . Recently, methods beyond conventional DFT, specifically the LDA+U method<sup>14</sup> as well as hybrid functionals<sup>15</sup>, have been used to study these structures, yielding in general satisfactory results. For example, the experimental band gap of pristine  $\text{TiO}_2$  is reproduced, and the relative stability of various vacancy charge states and the location of defect states in the band gap also agree well with experiments<sup>7, 16, 17</sup>.

The crystalline Magnéli phase  $\text{Ti}_4\text{O}_7$  has been shown experimentally to have a small energy gap ( $\sim 0.1$ - $0.2$  eV) below 142 K (low temperature, or LT), while it is metallic at room temperature (high temperature, or HT)<sup>18, 19</sup>. In contrast, theoretical approaches using LDA+U<sup>20, 21</sup> or hybrid functionals<sup>22</sup> predict a much larger energy gap (1.5 eV and 0.75 eV, respectively) than the experimentally measured one for the LT phase, and furthermore predict contradictory electronic structures for the HT phase. Liborio *et al.* used the B3LYP hybrid functional<sup>22</sup> and obtained an insulating antiferromagnetic (AF) HT phase with a band gap of 0.4 eV. On the other hand, Weissmann *et al.* used LDA+U, with value of U (0.4 Ry) determined by comparing the relative energies of different  $\text{Ti}_4\text{O}_7$  phases<sup>21</sup>, and obtained a ferromagnetic (FM) metallic phase. Weissman *et al.*<sup>21</sup> obtained an energy difference between the predicted ferromagnetic phase and a semiconducting AF state that is only 0.01 eV per formula unit. This energy difference is very low and would result in a mixture of different states at room temperature. It is desirable to have a single approach that can properly describe the electronic structures of the Magnéli phase as well as those of  $\text{TiO}_2$  and  $\text{Ti}_2\text{O}_3$ , considering that the Magnéli phase is positioned chemically between  $\text{TiO}_2$  and  $\text{Ti}_2\text{O}_3$ . In fact, this is of



great importance in the context of modeling  $\text{TiO}_2$ -based resistive switching devices, since not only  $\text{TiO}_2$  but also  $\text{Ti}_2\text{O}_3$  may coexist with the Magnéti phase<sup>10</sup> when oxygen atoms are removed from  $\text{TiO}_2$  as the material switches from high to low resistance state.

We have systematically modeled the electronic structures of the Magnéti phase  $\text{Ti}_4\text{O}_7$  together with the end members of the Magnéti phase, i.e.,  $\text{TiO}_2$  and  $\text{Ti}_2\text{O}_3$ , with the aim of describing these structures within the same approach. These titanium oxide phases cover a broad range of electronic properties, from metal (HT- $\text{Ti}_4\text{O}_7$ ) to narrow-gap semiconductor<sup>23, 24</sup> (band gap~0.1-0.2 eV, LT- $\text{Ti}_4\text{O}_7$  and  $\text{Ti}_2\text{O}_3$ ) and to insulator<sup>11,24</sup> (band gap~3 eV, rutile  $\text{TiO}_2$ ). Although the HT phase of  $\text{Ti}_4\text{O}_7$  is more relevant to devices, we also investigate the LT phase to validate the robustness of our approach. This is a sensitive test because a small difference in the crystal structure leads to significantly altered electronic properties<sup>25</sup>. In our work, we used the atomic-orbital-based self-interaction correction (ASIC) scheme<sup>26, 27</sup>. The amount of self-interaction correction is controlled by a single parameter,  $\alpha$ , which lies between 0 and 1 (for  $\alpha=1$  the full self-interaction correction is added, while for  $\alpha=0$  no correction is added). The  $\alpha$ -parameter empirically describes the charge screening in the given chemical environment. In metals with very good screening  $\alpha$  vanishes, while for highly ionic compounds with poor screening such as NaCl, a value of  $\alpha$  close to unity reproduces the experimental band gap<sup>26</sup>. For III-V and II-VI semiconductors as well as transition-metal oxides, the appropriate value of  $\alpha$  is shown to be typically around one half<sup>26</sup>. A central question regarding the ASIC methodology is then whether or not a single value of  $\alpha$  can be used to reasonably accurately describe all the different titanium oxides.

In order to search for the low-energy phases of  $\text{Ti}_4\text{O}_7$ , we have investigated the total energies of all possible collinear spin configurations for both the LT and HT phases. The results for a fixed  $\alpha$  value of 0.5, which is typically a reasonable value for transition metal oxides, are discussed in Sec. 3.1. In Sec. 3.2 we discuss varying  $\alpha$  to systematically investigate the dependence of the band gaps of LT- $\text{Ti}_4\text{O}_7$ ,  $\text{Ti}_2\text{O}_3$  and rutile  $\text{TiO}_2$  on  $\alpha$ . For the metallic HT- $\text{Ti}_4\text{O}_7$ , fixed spin moment calculations are performed at different  $\alpha$  values in order to include possible alignments of the magnetization. In devices for resistive switching, the presence of external electric fields or interfaces between different phases naturally induces structural deformations, i.e., strain, which may have a profound impact on the electronic properties of the materials involved. We have therefore looked into the effect of isotropic strain on the relative stability of different spin configurations for  $\text{Ti}_4\text{O}_7$  to predict its ground state under strain, and discuss our findings in Sec. 3.3.

## 2. Computational method

The DFT calculations are performed within the framework of the ASIC-LDA<sup>26, 27</sup>, as implemented in the SIESTA<sup>28</sup> electronic structure code. In a benchmark study<sup>27</sup> it was shown that the ASIC method is comparable to other advanced DFT methods (i.e., hybrid functionals and DFT+U) in delivering electronic structures, when applied to transition metal oxides such as MnO and NiO at equilibrium and under pressure. We use Troullier-Martins



pseudopotentials<sup>29</sup> and double- $\zeta$  basis sets with polarization functions for Ti and O atoms.  $\text{Ti}_4\text{O}_7$  has a triclinic structure with two pseudoorthorhombic sublattices<sup>30</sup>. Each unit cell consists of two formula units with a total of 22 atoms (Fig. 1). The equilibrium lattice parameters (Table I) and atomic coordinates of  $\text{Ti}_4\text{O}_7$  as well as  $\text{TiO}_2$  and  $\text{Ti}_2\text{O}_3$  are taken from experiments<sup>25, 31, 32</sup>. The SIESTA parameter ‘kgrid\_cutoff’, which sets the density of sampling k-points in the Brillouin zone<sup>33</sup>, is set to 30 Å to perform k-space integrations. This results in 486 points in the first Brillouin zone for  $\text{Ti}_4\text{O}_7$ . The unit cell volumes in real space are 232.7 Å<sup>3</sup> and 232.3 Å<sup>3</sup> for LT- $\text{Ti}_4\text{O}_7$  and HT- $\text{Ti}_4\text{O}_7$ , respectively.

TABLE I. Titanium oxides unit cell lattice parameters<sup>25, 31, 32</sup>.

	a	b	c	$\alpha$	$\beta$	$\gamma$
LT- $\text{Ti}_4\text{O}_7$	5.591 Å	6.915 Å	7.455 Å	120.64°	94.41°	104.52°
HT- $\text{Ti}_4\text{O}_7$	5.593 Å	6.899 Å	7.441 Å	120.56°	94.46°	104.35°
$\text{TiO}_2$	4.594 Å	4.594 Å	2.958 Å	90°	90°	90°
$\text{Ti}_2\text{O}_3$	5.433 Å	5.433 Å	5.433 Å	56.75°	56.75°	56.75°

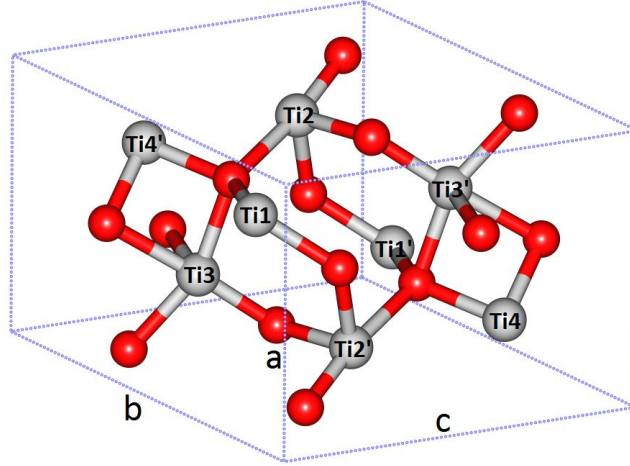


Figure 1. Atomic structure of  $\text{Ti}_4\text{O}_7$  crystal unit cell. Grey spheres represent titanium and red spheres represent oxygen atoms. The numbering of Ti atoms is also shown.

### 3. Results and discussion

#### 3.1 $\text{Ti}_4\text{O}_7$ ground state spin configuration

We study  $\text{Ti}_4\text{O}_7$  using a fixed value of the ASIC parameter  $\alpha = 0.5$  at two experimentally determined atomic structures given in Table I. We will in fact show in Sec. 3.2 that  $\alpha = 0.5$  successfully reproduces the energy gap for the LT phase, and also reasonably well describes the metallic properties of the HT phase. It is well established<sup>21, 22, 25, 34</sup> that  $\text{Ti}_4\text{O}_7$  exhibits charge localization at the metal-insulator transition. In the HT phase all Ti atoms have uniform charges<sup>22, 25</sup> (+3.5), as evidenced by the similar average Ti-O distances (2.01 - 2.02 Å) for all Ti atoms. By comparing measured Ti-O distances and tabulated ionic radii these Ti atoms were found<sup>22</sup> to have a charge of +3.5. Delocalization of the Ti 3d electrons



leads to metallic properties of the HT phase. In contrast, in the LT phase the Ti atoms can be classified into two groups:  $\text{Ti}^{3+}$  (Ti1, Ti1', Ti3 and Ti3' in Fig. 1) and  $\text{Ti}^{4+}$  (Ti2, Ti2', Ti4 and Ti4') ions. The corresponding average Ti-O distances are 2.04 Å for  $\text{Ti}^{3+}$  ions, and 1.97/2.00 Å for  $\text{Ti}^{4+}$  ions, respectively. Furthermore, long-range ordering of  $\text{Ti}^{3+}$ - $\text{Ti}^{3+}$  pairs leads to charge localization for the LT phase, which in turn causes semiconducting properties. Regarding the details of chemical bonding in  $\text{Ti}_4\text{O}_7$ , previous spin-resolved electronic structure calculations have yielded contradictory conclusions<sup>21,22</sup>, as discussed in the Introduction.

As shown in Fig. 1, 8 Ti atoms within one unit cell correspond to two sublattices, with 4 Ti atoms in each sublattice. We use the same numbering (e.g., Ti1 and Ti1') to denote the Ti atoms related by point group symmetry in the two sublattices, with the atoms in the second sublattice denoted by a prime sign. References 21 and 22 both considered only ferromagnetic coupling between the two sublattices, such that Ti1 and Ti1' had the same magnetic moment, as did Ti2 and Ti2' and so on. However, we note that the structural symmetry between the two sublattices is conserved by both ferromagnetic and antiferromagnetic coupling.

TABLE II. Total energies (per formula unit), magnetic moments (per formula unit), band gaps and Ti atomic spins estimated by Mulliken population analysis of different spin configurations of  $\text{Ti}_4\text{O}_7$  at  $\alpha = 0.5$ . Note that each unit cell consists of two formula units.

		HT			LT			
Spin state		FM	AF1	AF2	FM	AF1	AF2	AF3
Energy (eV)		-0.171	-0.095	-0.100	-0.230	-0.282	-0.213	-0.300
Moment ( $\mu_B$ )		2	0	0	2	0	0	0
Band gap (eV)		0	0	0	0	0.23	0.11	0.34
Atomic spin ( $\mu_B$ )	Ti1	+0.561	+0.060	-0.059	+0.897	+0.785	+0.885	+0.783
	Ti2	+0.709	+0.647	+0.656	+0.257	-0.005	-0.073	+0.025
	Ti3	+0.536	+0.211	-0.421	+0.830	-0.742	+0.776	-0.733
	Ti4	+0.552	-0.523	+0.378	+0.336	-0.040	-0.067	-0.003
	Ti1'	+0.561	-0.060	+0.059	+0.897	+0.785	-0.885	-0.783
	Ti2'	+0.709	-0.647	-0.656	+0.257	-0.005	+0.073	-0.025
	Ti3'	+0.536	-0.211	+0.421	+0.830	-0.742	-0.776	+0.733
	Ti4'	+0.552	+0.523	-0.378	+0.336	-0.040	+0.067	+0.003

In order to determine the ground state spin configuration, we explore all possible spin configurations that respect structural symmetry. Explicitly, we consider all  $8=2^4/2$  (flipping all atomic spins simultaneously returns the same state) possible spin configurations across 4 Ti atoms within each sublattice (++++, +++-, ++--, ..., +---), as well as both FM and AF coupling between the two sublattices. Thus, we consider all 16 possible collinear spin states within a unit cell. After the total energies converge self-consistently, we find that some initial spin configurations are transformed to other states, indicating that they do not correspond to a metastable local minimum in energy. In all, we find three stable spin-polarized solutions for the HT-phase (one FM state and two AF states), and four stable solutions for the LT-phase (one FM state and three AF states) (Table II). For the LT phase, both the non-magnetic state and FM state have vanishing band gaps, which is inconsistent with experiments. The AF1



(Table II) state is very similar (see Appendix) to the ground state obtained by either the B3LYP hybrid functional<sup>22</sup> or the LDA+U approach<sup>21</sup>, which has an AF coupling between Ti1 and Ti3 (and between Ti1' and Ti3'), and with an FM coupling between two sublattices. However, by comparing total energies (Table II) we find that the ground state corresponds to a state in which the two sublattices are coupled antiferromagnetically (AF3 in Table II), and not ferromagnetically. In this state the magnetic moments for Ti1 (Ti1') and Ti3 (Ti3') are +0.783 (-0.783) and -0.733 (+0.733)  $\mu_B$ , respectively. The magnetic moments for all other Ti atoms are on the other hand negligible (less than 0.1  $\mu_B$ ). Compared to the AF1 state that was previously argued<sup>21, 22</sup> to be the ground state, the AF coupling between two sublattices explored in this work further reduces the total energy by 0.037 eV per unit cell, yielding the global energy minimum. To check the robustness of this result, we vary  $\alpha$  from 0.45 to 0.7, which yields band gaps between 0 and 1 eV for both AF1 and AF3 states. We have confirmed that in this range of  $\alpha$  AF3 is always energetically preferred to AF1 (see Figure A2 in the Appendix).

For the HT phase,  $\alpha = 0.5$  results in a ferromagnetic ground state. All Ti atoms have similar atomic spins (0.5 - 0.7  $\mu_B$ ), with a total magnetic moment of 2  $\mu_B$  per formula unit. Note that we use Mulliken population analysis to estimate atomic spin; some oxygen atoms have small but non-zero opposite spins such that the total spin for one  $\text{Ti}_4\text{O}_7$  formula unit is 2  $\mu_B$ . Our result is similar to the FM state predicted by Weissmann<sup>21</sup> (LDA+U), which, however, was not the lowest-energy state in that work. We will further address this issue in Sec. 3.2, where we will discuss results of fixed spin moment calculations.



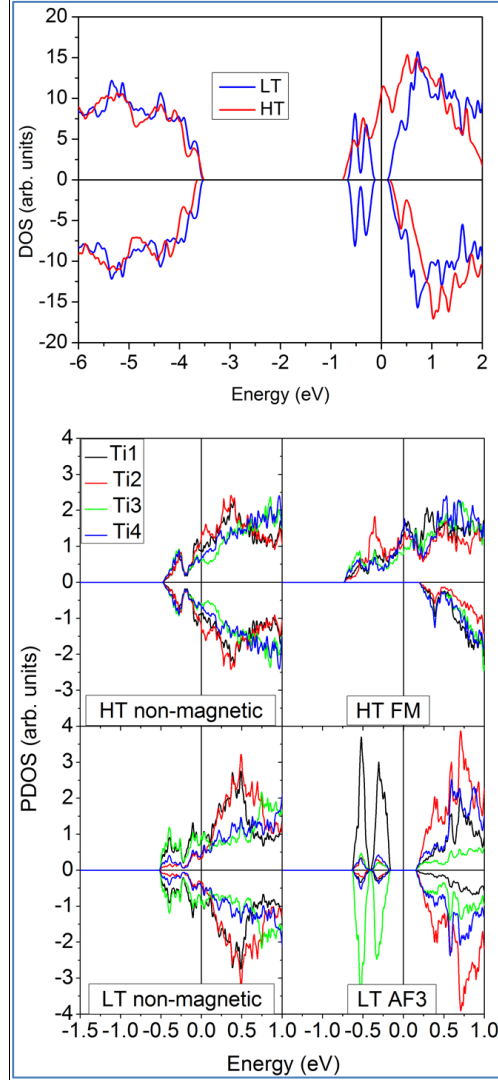


Figure 2. Upper panel: the low-energy state density of states (DOS) of LT- and HT- $\text{Ti}_4\text{O}_7$  at  $\alpha = 0.5$ . Lower panel: the atom-resolved projected DOS (PDOS) of one sublattice of  $\text{Ti}_4\text{O}_7$  for non-magnetic solutions and ground states. The numbering of Ti atoms can be found in Fig. 1 and Table II. The Fermi level is set to zero in all plots (see discussion in text).

The electronic densities of states for LT and HT phases of  $\text{Ti}_4\text{O}_7$  are shown in Fig. 2. The total DOS of the low-energy states are shown in the upper panel. For the LT phase the ground state is the AF3 state. It shows that AF coupling between two sublattices results in degenerate total DOS for both spin components, as expected. The predicted band gap of  $\sim 0.3$  eV is slightly higher than the experimentally measured ones ( $\sim 0.1$ - $0.2$  eV<sup>18, 19</sup>), while previous LDA+U or hybrid functional calculations deviate more<sup>21, 22</sup>. It should be noted that the Fermi level,  $E_f$  (energy zero in Fig. 2), in a DFT calculation is arbitrarily located within the band gap for an intrinsic semiconductor. Taguchi *et al.* have recently performed photoemission spectroscopy (PES) study<sup>19</sup> on  $\text{Ti}_4\text{O}_7$ . They concluded that the Fermi level is located at or near the conduction band minimum for all phases. The DOS projected on Ti atoms is shown in the lower panel of Fig. 2. The non-magnetic projected DOS (PDOS) can be used as a reference point before spin polarization is considered. For the LT phase, the non-magnetic PDOS just below  $E_f$  is dominated by the paired  $\text{Ti}^{3+}$  ions (Ti1 and Ti3), which have the smallest Ti-Ti



distance (2.802 Å). The AF coupling between Ti1 and Ti3 in the AF3 state induces localized states giving rise to sharp peaks below  $E_f$ . These localized states effectively open up a finite gap, accompanied by a reduction of the total energy. Compared with the previously assumed ground state (AF1), the AF coupling across the two sublattices actually enhances the separation between these localized states and conduction band, further reducing total energy by 0.037 eV/unit cell. For the HT phase the low-energy state is the FM state. Both the non-magnetic reference state and the FM low-energy state show similar DOS among all Ti atoms, reflecting similar chemical environments for the Ti atoms. Near  $E_f$ , FM coupling induces full spin polarization up to  $\sim 0.2$  eV above  $E_f$ , leading to half-metallic properties.

### 3.2 The effect of varying the ASIC parameter $\alpha$

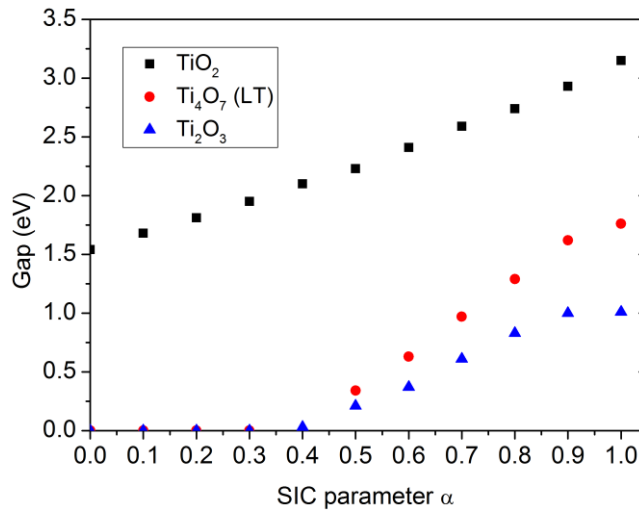


Figure 3. Predicted band gap vs. empirical parameter  $\alpha$  for LT- $\text{Ti}_4\text{O}_7$ ,  $\text{TiO}_2$  and  $\text{Ti}_2\text{O}_3$ .

In section 3.1 we have discussed the electronic/magnetic properties of  $\text{Ti}_4\text{O}_7$  for fixed  $\alpha = 0.5$ , which reproduces the value of the band gap for many oxides<sup>26</sup>. Our results are consistent with this finding in that they are in good agreement with experiment, i.e., the predicted band gap of the LT phase is comparable to the experimental one, and for the HT phase the metallicity is reproduced. The value of  $\alpha$  is expected to vary from one material to another, reflecting the fact that  $\alpha$  is directly related to the screening properties of a given material. We therefore need to ascertain whether the ASIC method with the same value of  $\alpha$  can be used for different Ti oxides as formed during resistive switching, in which fluctuations in the external environment lead to changes in material structures and properties. One way to check this is to apply the same method as we used for  $\text{Ti}_4\text{O}_7$  to rutile  $\text{TiO}_2$  and  $\text{Ti}_2\text{O}_3$ , in which titanium and oxygen are subject to different chemical environment as a result of different stoichiometry. To check the robustness of the applied ASIC method, we have systematically studied the variation of band gaps of  $\text{Ti}_4\text{O}_7$  together with  $\text{TiO}_2$  and  $\text{Ti}_2\text{O}_3$  as a function of  $\alpha$  (Fig. 3), all of which may coexist in a  $\text{TiO}_2$ -based structure for resistive switching.

All three materials exhibit a nearly linear relationship between band gap and  $\alpha$  in the regions of  $\alpha$  with non-zero band gaps as shown in Figure 3. This is consistent with previous ASIC



benchmark work<sup>26</sup>. The only exception is at  $\alpha = 1$ , for which ASIC is applied at full strength yielding an unphysically large band gap for both LT-Ti<sub>4</sub>O<sub>7</sub> and Ti<sub>2</sub>O<sub>3</sub>. When  $\alpha$  is set to the ‘typical’ value of 0.5, the predicted band gaps for LT-Ti<sub>4</sub>O<sub>7</sub>, Ti<sub>2</sub>O<sub>3</sub> and TiO<sub>2</sub> are 0.34 eV, 0.21 eV and 2.23 eV, respectively. The experimental band gaps for both LT-Ti<sub>4</sub>O<sub>7</sub> and Ti<sub>2</sub>O<sub>3</sub> are about 0.1-0.2 eV<sup>18, 19, 23, 24</sup>, which can be exactly reproduced by setting  $\alpha$  to a value in between 0.4 and 0.5 (Fig. 3). It is interesting to note that although Ti<sub>2</sub>O<sub>3</sub> is non-magnetic<sup>35</sup> and LT-Ti<sub>4</sub>O<sub>7</sub> has an AF ground state, both materials have very similar band gaps, which are both captured by the ASIC scheme. On the other hand, while  $\alpha = 0.5$  yields quite reasonable band gaps for these two narrow-gap semiconductors, a larger  $\alpha$  value of  $\sim 0.9$  is required to quantitatively reproduce band gap for the insulating rutile TiO<sub>2</sub> ( $\sim 3.0$  eV). This is reasonable from the point of view that in TiO<sub>2</sub> all Ti atoms have a valence charge of +4, representing a more ionic system with reduced electronic screening of charges.

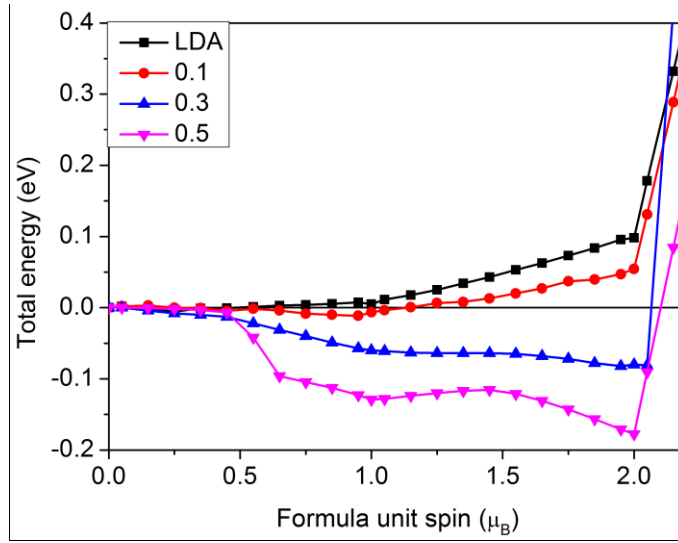


Figure 4. Total energy per formula unit of HT-Ti<sub>4</sub>O<sub>7</sub> as a function of magnetization for  $\alpha=0$  (black squares),  $\alpha=0.1$  (red circles),  $\alpha=0.3$  (blue triangles), and  $\alpha=0.5$  (pink downward-pointing triangles). The total energy at zero spin is used as a reference for each value of  $\alpha$ .

We have shown in section 3.1 that  $\alpha = 0.5$  yields half-metallic properties for HT-Ti<sub>4</sub>O<sub>7</sub>. Although the gapless state is consistent with experiments, a ferromagnetic low-energy state appears to be questionable. Magnetic susceptibility measurements suggest that Ti<sub>4</sub>O<sub>7</sub> is Pauli-paramagnetic<sup>18</sup> at room temperature, rather than ferromagnetic, although it has been suggested<sup>19</sup> that a low-moment FM state can lead to apparent paramagnetism. On the other hand the value of  $\alpha = 0.5$  for HT-Ti<sub>4</sub>O<sub>7</sub> might be too large, since it is essentially a metal and therefore already screens effectively. Thus, it is interesting to examine the dependency of magnetic properties on the value of  $\alpha$ . The behavior of energy vs. magnetization is calculated by fixed spin moment calculations (Fig. 4). The LDA result corresponds to  $\alpha = 0$ , and shows a monotonic increase of energy with magnetization, implying a paramagnetic property in agreement with experiments. When  $\alpha$  increases from 0 to 0.5, the total energy is gradually reduced with increasing magnetization, indicating a higher and higher tendency of spontaneous magnetization (ferromagnetism). Consequently, one can infer that  $\alpha = 0$



results in a better description for HT-Ti<sub>4</sub>O<sub>7</sub>, although  $\alpha = 0.5$  also predicts a gapless DOS at the Fermi energy. For  $\alpha = 0.5$  each Ti atom shows a maximum reduced energy of 0.044 eV (0.18 eV per formula unit) upon magnetization (at 2  $\mu_B$  per formula unit, Fig.4). Beyond 2  $\mu_B$  per formula unit, the magnetization exceeds the value that can be obtained by aligning all Ti 3d electron spins in the same direction (in the HT phase each Ti ion has a valence charge of +3.5 and there are 4 Ti atoms per formula unit), leading to a rapid increase in energy.

We close this section with a comment on the selection of  $\alpha$  in modeling TiO<sub>2</sub>-based switching structures. On one hand, we have shown that in order to match ‘exactly’ experimentally measured electrical and magnetic properties,  $\alpha$  needs to be adjusted for different titanium oxide phases. The measured band gaps for HT-Ti<sub>4</sub>O<sub>7</sub>, LT-Ti<sub>4</sub>O<sub>7</sub>, Ti<sub>2</sub>O<sub>3</sub> and TiO<sub>2</sub> are 0 eV, 0.1-0.2 eV, 0.1-0.2 eV and 3 eV, respectively, partly reflecting different screening strengths intrinsic to the materials. Correspondingly, the ‘best’ values of the modeling parameter  $\alpha$  are found to be 0, ~0.5, ~0.5 and ~0.9, respectively. A similar situation may also apply to the LDA+U approach or hybrid functionals in case one wishes to model all of the important titanium oxide phases in resistive switching devices using a single method. The LDA+U approach applies on-site Coulomb corrections to some orbitals, while hybrid functional mixes some portion of Hartree-Fock exchange with conventional exchange and correlation. Different values of U or Hartree-Fock exchange may be needed in order to match, e.g., band gap to experimental values, which then leads to the question of how to model the whole sequence of Ti oxides using a single parameter set. On the other hand, within the ASIC method, a single value for  $\alpha$  of 0.5, which is about the average of the desired values, can be chosen to semi-quantitatively model all these phases, yielding band gaps of 0 eV, 0.34 eV, 0.21 eV and 2.23 eV, respectively. Consequently, we expect that ASIC at  $\alpha = 0.5$  can reasonably well model electronic transport properties, which are determined by the overall electronic structure, of a heterostructure formed by different Ti-O phases. The main point in this case is to capture reasonably well the density of states and the character of the band gap; for  $\alpha = 0.5$ , TiO<sub>2</sub> retains 74% value of its band gap, while HT-Ti<sub>4</sub>O<sub>7</sub> remains gapless.

### 3.3 Evolution of spin states with applied strain.

All calculations presented in sections 3.1 and 3.2 are based on experimental structures. For the transition metal oxides MnO and NiO, it was found that LDA+ASIC underestimates the experimental lattice constant<sup>27</sup> by ~2%. It was also shown in the same work that the electronic spin polarization depends critically on the lattice constant, i.e., strain. Table II shows that the total energy differences between some spin states of Ti<sub>4</sub>O<sub>7</sub> are relatively small (< 0.1 eV), which may lead to a strain-induced magnetic phase transition<sup>27</sup>. This is an issue that needs to be considered, because strain fields are expected to be present in resistive switching devices due to the presence of, e.g., external electric fields or interfaces.



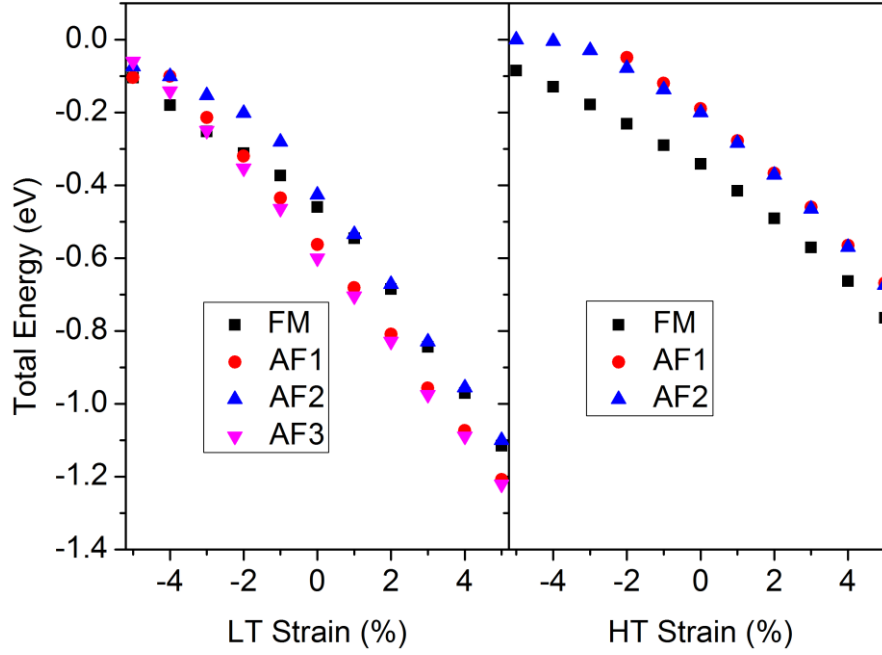


Figure 5. Total energy of different spin configurations of  $\text{Ti}_4\text{O}_7$  as a function of isotropic strain. The total energies of the corresponding non-magnetic solutions are set as reference points.

The evolution of total energies of different spin configurations (relative to the respective non-magnetic LT and HT states) as a function of isotropic strain is shown in Fig. 5. Isotropic strain is modeled by varying atomic coordinates (and lattice constants) proportionally in all directions. It is clear from the figure that spin polarization always lowers the total energy compared to non-polarized states. When compressive strain is applied, all magnetic states gradually converge to non-magnetic states. At (an unrealistically large) strain of -12%, the spin polarization vanishes for all states of both LT and HT phases (not shown). There appears to be a magnetic phase transition (AF3 to FM) for the LT phase at a more realistic strain of -3%. For the HT phase the FM state is always the ground state in the whole range of modeled strain.

## 4. Conclusions

In summary, we have systematically used the LDA-ASIC approach to study the  $\text{Ti}_4\text{O}_7$  Magnéli phase, as well as  $\text{Ti}_2\text{O}_3$  and rutile  $\text{TiO}_2$ . By searching throughout the possible spin configurations at  $\alpha = 0.5$ , we show that the ground state for the LT phase is a novel antiferromagnetic state (AF3), with a calculated band gap of  $\sim 0.3$  eV. The HT phase is a metal irrespective of the spin configuration. By performing fixed spin moment calculations we show that HT- $\text{Ti}_4\text{O}_7$  tends to be ferromagnetic for finite  $\alpha$ , and becomes Pauli paramagnetic for vanishing  $\alpha$ . The experimental band gaps of LT- $\text{Ti}_4\text{O}_7$  and  $\text{Ti}_2\text{O}_3$  can be reasonably well reproduced with  $\alpha \gg 0.5$ , while the more ionic wide-gap  $\text{TiO}_2$  needs larger  $\alpha$  ( $\sim 0.9$ ) to recover the correct gap. However, we conclude that a single value of  $\alpha = 0.5$  may adequately describe these three oxides. This is an important point, as it will enable modeling of structures such as those in resistive switching, in which all three oxides may be



present. By modeling  $\text{Ti}_4\text{O}_7$  under isotropic strain for  $\alpha = 0.5$ , we find that the FM state is always the ground state for the HT phase while there appears to be an AF-FM phase transition for the LT phase under a moderate compressive strain.

## Appendix: a comparison between LT- $\text{Ti}_4\text{O}_7$ AF1 and AF3 states

Our LT-AF1 state is very similar to the ground state predicted by either the LDA+U method<sup>21</sup> or by hybrid functional<sup>22</sup>, as shown in Figure A1. In this state two sublattices of  $\text{Ti}_4\text{O}_7$  are ferromagnetically coupled, while Ti1 and Ti3 (or Ti1'' and Ti3') are antiferromagnetically coupled. Although the total magnetization is zero, spin up DOS and spin down DOS are not degenerate. On the other hand, the two spin components are degenerate in our LT-AF3 ground state, as a result of AF coupling between two sublattices.

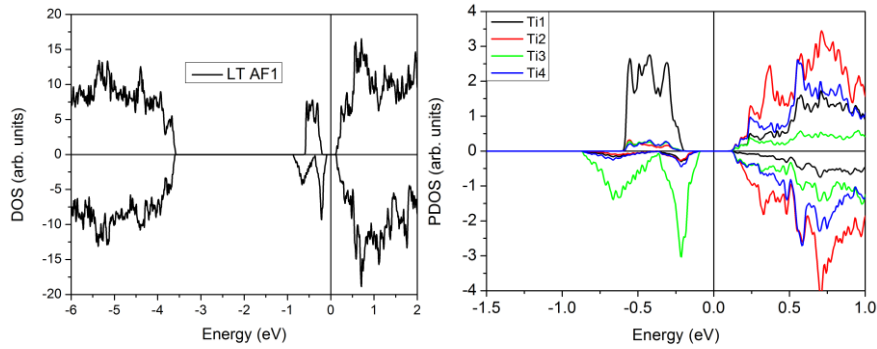


Figure A1. Total DOS (left) and PDOS (right) projected on the first sublattice of  $\text{Ti}_4\text{O}_7$  LT-AF1 state at  $\alpha = 0.5$ .

To ascertain if AF3 is the ground state we checked the relative stability of AF3 vs. AF1 (Figure A2). Figure A2 shows that in the relevant band gap region ( $\sim 0 - \sim 1$  eV) AF3 always has a lower energy and a slightly larger band gap (about 0.1 eV) compared with AF1. The band gap of 0.1-0.2 eV of LT- $\text{Ti}_4\text{O}_7$  can be exactly reproduced by  $\alpha \approx 0.45$ , where AF3 has a lower energy of about 0.021 eV/formula unit than AF1.

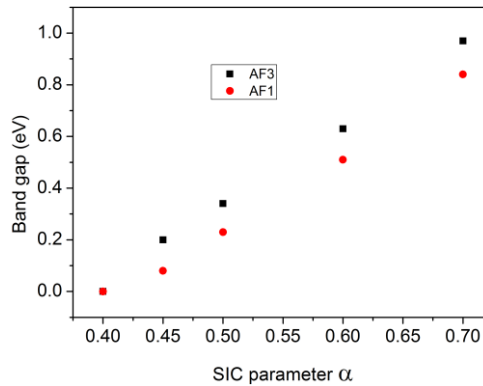


Figure A2. Left: total energy difference as  $E_{\text{AF3}} - E_{\text{AF1}}$  per formula unit for LT- $\text{Ti}_4\text{O}_7$ . Right: band gap vs.  $\alpha$  for both AF1 and AF3 states.



## References:

- [1] B. Oregan and M. Gratzel, *Nature* **353**, 737 (1991).
- [2] K. Hashimoto, H. Irie, and A. Fujishima, *Jpn. J. Appl. Phys.* **44**, 8269 (2005).
- [3] D. B. Strukov, G. S. Snider, D. R. Stewart, and R. S. Williams, *Nature* **453**, 80 (2008).
- [4] J. J. Yang, M. D. Pickett, X. Li, A. A. Ohlberg, D. R. Stewart, and R. S. Williams, *Nat. Nanotechnol.* **3**, 429 (2008).
- [5] J. Doo Seok, T. Reji, R. S. Katiyar, J. F. Scott, H. Kohlstedt, A. Petraru, and H. Cheol Seong, *Rep. Prog. Phys.* **75**, 076502 (2012).
- [6] J. P. Strachan, M. D. Pickett, J. J. Yang, S. Aloni, A. L. David Kilcoyne, G. Medeiros-Ribeiro, and R. Stanley Williams, *Adv. Mater.* **22**, 3573 (2010).
- [7] S. G. Park, B. Magyari-Köpe, and Y. Nishi, *Phys. Rev. B* **82**, 115109 (2010).
- [8] L. Zhao, S. G. Park, B. Magyari-Köpe, and Y. Nishi, *Math. Comput. Model.* **58**, 275 (2013).
- [9] D. H. Kwon *et al.*, *Nat. Nanotechnol.* **5**, 148 (2010).
- [10] J. J. Yang, J. Strachan, F. Miao, M. X. Zhang, M. Pickett, W. Yi, D. A. Ohlberg, G. Medeiros-Ribeiro, and R. S. Williams, *Appl. Phys. A* **102**, 785 (2011).
- [11] A. L. Linsebigler, G. Lu, and J. T. Yates, *Chem. Rev.* **95**, 735 (1995).
- [12] M. Landmann, E. Rauls, and W. G. Schmidt, *J. Phys.: Condens. Matter* **24**, 195503 (2012).
- [13] E. Cho, S. Han, H. S. Ahn, K. R. Lee, S. K. Kim, and C. S. Hwang, *Phys. Rev. B* **73**, 193202 (2006).
- [14] S. L. Dudarev, G. A. Botton, S. Y. Savrasov, C. J. Humphreys, and A. P. Sutton, *Phys. Rev. B* **57**, 1505 (1998).
- [15] J. Heyd, G. E. Scuseria, and M. Ernzerhof, *J. Chem. Phys.* **118**, 8207 (2003).
- [16] A. Janotti, J. B. Varley, P. Rinke, N. Umezawa, G. Kresse, and C. G. Van de Walle, *Phys. Rev. B* **81**, 085212 (2010).
- [17] P. Deák, B. Aradi, and T. Frauenheim, *Phys. Rev. B* **86**, 195206 (2012).
- [18] S. Lakkis, C. Schlenker, B. K. Chakraverty, R. Buder, and M. Marezio, *Phys. Rev. B* **14**, 1429 (1976).
- [19] M. Taguchi *et al.*, *Phys. Rev. Lett.* **104**, 106401 (2010).
- [20] I. Leonov, A. N. Yaresko, V. N. Antonov, U. Schwingenschlögl, V. Eyert, and V. I. Anisimov, *J. Phys.: Condens. Matter* **18**, 10955 (2006).
- [21] M. Weissmann and R. Weht, *Phys. Rev. B* **84**, 144419 (2011).
- [22] L. Liborio, G. Mallia, and N. Harrison, *Phys. Rev. B* **79**, 245133 (2009).
- [23] T. C. Chi and R. J. Sladek, *Phys. Rev. B* **7**, 5080 (1973).
- [24] G. Yuzheng, J. C. Stewart, and R. John, *J. Phys.: Condens. Matter* **24**, 325504 (2012).
- [25] M. Marezio, D. B. McWhan, P. D. Dernier, and J. P. Remeika, *J. Solid State Chem.* **6**, 213 (1973).
- [26] C. D. Pemmaraju, T. Archer, D. Sánchez-Portal, and S. Sanvito, *Phys. Rev. B* **75**, 045101 (2007).
- [27] T. Archer *et al.*, *Phys. Rev. B* **84**, 115114 (2011).
- [28] M. S. José *et al.*, *J. Phys.: Condens. Matter* **14**, 2745 (2002).
- [29] N. Troullier and J. L. Martins, *Phys. Rev. B* **43**, 1993 (1991).
- [30] J. L. Hodeau, M. Marezio, C. Schlenker, R. Buder, and S. Lakkis, *J. Appl. Crystallogr.* **9**, 391 (1976).
- [31] International Tables for Crystallography, Space-Group Symmetry, ed. T. Hahn (Springer, New York, 2005) 5th ed., Vol. A.
- [32] W. R. Robinson, *J. Solid State Chem.* **9**, 255 (1974).
- [33] J. Moreno and J. M. Soler, *Phys. Rev. B* **45**, 13891 (1992).
- [34] M. Marezio, D. B. McWhan, P. D. Dernier, and J. P. Remeika, *Phys. Rev. Lett.* **28**, 1390 (1972).



[35] R. M. Moon, T. Riste, W. C. Koehler, and S. C. Abrahams, J. Appl. Phys. **40**, 1445 (1969).